SPACE RESEARCH COORDINATION CENTER

MEASUREMENTS OF O(^{1}D) QUENCHING RATES IN THE F-REGION

BY

DWIGHT P. SIPLER AND MANFRED A. BIONDI

SRCC REPORT NO. 170

UNIVERSITY OF PITTSBURGH

PITTSBURGH, PENNSYLVANIA

APRIL 1972

The Space Research Coordination Center, established in May, 1963, has the following functions: (1) it administers predoctoral and postdoctoral fellowships in space-related science and engineering programs; (2) it makes available, on application and after review, allocations to assist new faculty members in the Division of the Natural Sciences and the School of Engineering to initiate research programs or to permit established faculty members to do preliminary; work on research ideas of a novel character; (3) in the Division of the Natural Sciences it makes an annual allocation of funds to the Interdisciplinary Laboratory for Atmospheric and Space Sciences; (4) in the School of Engineering it makes a similar allocation of funds to the Department of Metallurgical and Materials Engineering and to the program in Engineering Systems Management of the Department of Industrial Engineering; and (5) in concert with the University's Knowledge Availability Systems Center, it seeks to assist in the orderly transfer of new space-generated knowledge in industrial application. The Center also issues periodic reports of space-oriented research and a comprehensive annual report.

The Center is supported by an Institutional Grant (NsG-416) from the National Aeronautics and Space Administration, strongly supplemented by grants from the A. W. Mellon Educational and Charitable Trust, the Maurice Falk Medical Fund, the Richard King Mellon Foundation and the Sarah Mellon Scaife Foundation. Much of the work described in SRCC reports is financed by other grants, made to individual faculty members.

APP-29

Measurements of $O(^1D)$ Quenching Rates in the F-Region

(Journal of Geophysical Research)

Dwight P. Sipler and Manfred A. Biondi

University of Pittsburgh

Pittsburgh, Pennsylvania 15213

April 1972

Measurements of $O(^1D)$ Quenching Rates in the F-Region

Dwight P. Sipler and Manfred A. Biondi
Physics Dept., University of Pittsburgh
Pittsburgh, Pa. 15213

Abstract

In-situ determinations of the quenching of $O(^1D)$ atoms by N_2 and O_2 molecules have been made from observations of 6300A nightglow intensity enhancements produced by the Platteville 1.6 Mw transmitter. The heating of F-region electrons near the point of reflection of the rf wave leads to electron impact excitation of oxygen atoms to the $O(^1D)$ state. It is shown that the resulting region of enhanced 6300A emission is localized to the region of electron energy absorption for heating at the lower altitudes. At 225 km the measured time constants for intensity buildup following transmitter turn-on and for intensity decay following turn-off are identical and equal to (13 ± 1) sec. Time constants varying from 30 - 80 sec are found for the altitude range 260-300 km. The inferred quenching coefficient for the whole altitude range, 225-300 km, is $k_q = (4.4 \pm \frac{2}{1}) \times 10^{-11}$ cm^3/sec at 950^oK, in good agreement with laboratory data. The quenching frequency obtained at 225 km, when referred to the altitude 120 km, is equal to (21 ± 2) sec^{-1}, in agreement with less direct ionospheric determinations

Introduction

The natural lifetime (110 sec) of the metastable $O(^1D)$ state is expected to be significantly shortened by quenching collisions in the Earth's ionosphere at altitudes below ~ 350 km. This expectation is based upon a consideration of laboratory measurements of the relevant quenching coefficients, e.g., $k_q(N_2) = (5 \pm 2) \times 10^{-11}$ and $k_q(O_2) = (6 \pm 2) \times 10^{-11}$ cm^3/sec at 300^oK [Clark and Noxon, 1972; Noxon , 1970; Young et al., 1968], and the expected height distribution of the quenching molecules. However, there is very little direct information concerning the $O(^1D)$ lifetime in the ionosphere; one example is the measurements of Peterson and van Zandt [1969], in which changes in the 6300A ($^1D \rightarrow {}^3P$) nightglow intensity were correlated with F-region electron density and emitting layer height changes to obtain an average of the $O(^1D)$ lifetime over the emitting region.

The recent use of powerful ground-based transmitters to produce significant increases in the energy of the electrons in the F region [Utlaut, 1970; Gordon , et al., 1971] has provided a means for carrying out experiments involving controlled changes in the ionosphere. These changes can then be compared with predictions derived from a model which includes those processes which are believed to be significant in determining the ionospheric behavior. As an example, observations of transient 6300A intensity changes were successfully correlated with a model of the production of $O(^1D)$ atoms in the F-region [Biondi et al., 1970]. This model is based on the production of O_2^+ ions by the $O^+ + O_2$ charge transfer reaction, followed by $O(^1D)$ production by the $O_2^+ + e$ dissociative recombination reaction. In this model, the $O(^1D)$ lifetime and the dissociative recombination lifetime determine the shape of the intensity transient. Inasmuch as the 6300A intensity transients produced to date have been very weak, no accurate determi-

nations of $O(^1D)$ lifetimes have been obtained from these measurements.

In later experiments performed in conjunction with the Platteville, Colo. transmitter operating in a more efficient heating mode [Utlaut and Cohen, 1971] much stronger 6300A intensity changes have been produced, apparently as a result of impact excitation of $O(^3P)$ atoms by fast electrons. In this case the $O(^1D)$ state lifetime enters simply and directly in the analysis, and hence we have been able to determine the lifetime with reasonable accuracy from our observations of 6300A intensity changes [Sipler and Biondi, 1971].

The geometry of the experiment is shown schematically in Figure 1. The 1.6 Mw c-w transmitter, capable of operating at frequencies between 5.3 and 10 MHz, is located at Platteville, Colo. (near Denver). Circularly polarized waves are projected vertically from the antenna array and are bent by the magneto-plasma (the ionosphere in the Earth's magnetic field), the "ordinary" circular polarization (O-mode) bending north until it is normal to the Earth's magnetic field (dip angle, 68°) at the point of reflection. The "extraordinary" circular polarization (X-mode) is bent southward until it parallels the magnetic field at the point of reflection. From the maps of electron temperature change produced by the Arecibo heating transmitter [Gordon et al., 1971] it appears that the heated electron region is sometimes rather localized to the reflection point of the wave (within some tens of km), showing slight elongation along the magnetic field due to the higher electron conductivity along the field lines. Thus, the radiation from the $O(^1D)$ atoms produced by electron impact excitation of oxygen atoms may be sufficiently localized in altitude in these experiments that a single lifetime can be used to characterize the emitting states. In this case the analysis of the 6300A intensity changes produced by the rf transmitter provides a direct measurement of the $O(^1D)$ lifetime in the vicinity of the

reflection point of the rf wave.

In the next sections, we discuss the processes leading to 6300A radiation in these experiments, describe the photometer apparatus used to measure the 6300A intensity changes, give examples of the data obtained, and analyze the data to infer the $O(^1D)$ lifetime as a function of altitude. We then combine these results with a model of the neutral atmosphere's composition to obtain the quenching coefficient by N_2 and O_2 molecules.

Processes Leading to 6300A Radiation

We consider the production and loss of $O(^1D)$ atoms in a quiet, nighttime ionosphere periodically irradiated by a radio frequency wave which is reflected (and partially absorbed) at some point in the F_2 region. The effect of the rf wave is to impart energy to the electrons in the F-region; the electrons reach a new quasi-stationary energy distribution in the presence of the heating wave on a time scale which is usually short compared to the times of interest in our analysis [Meltz and LeLevier, 1970]. Thus, the differential equation governing the concentration of $O(^1D)$ atoms may be written in the form:

$$\partial[^1D]/\partial t = Q_r + Q_x - (1/\tau_n)[^1D] - 1.1\, k_q\, [N_2][^1D] + D_x \nabla^2[^1D], \qquad (1)$$

where the [] brackets indicate particle concentrations. The source term resulting from dissociative recombination between O_2^+ ions and electrons,

$$Q_r = \alpha(^1D)\, n_e\, [O_2^+], \qquad (2)$$

depends on the effective recombination coefficient, $\alpha(^1D)$, for production of the ^1D states directly and by cascading from higher lying states. Zipf [1970] has shown that at 300°K ~ 1.0 (^1D) states are produced per electron captured by O_2^+. (A similar term may possibly be needed to account for ^1D production by recombination with NO^+ ions but has not been included.) As noted above, this source term (2) appears to account for the 6300A radiation from the nightglow and its variation with rf heating observed in our earlier experiment [Biondi, et al., 1970].

When a sufficient number of electrons receive energies exceeding ~ 2 eV from the rf heating, impact excitation of ambient oxygen atoms leads to significant production of the ^1D states; this source term may be represented by

$$Q_x = [O]n_e \int_o^\infty f(\varepsilon)\, \sigma_x(\varepsilon) v\, d\varepsilon \qquad (3)$$

where $f(\varepsilon)$ is the normalized energy distribution of the electrons, $\sigma_x(\varepsilon)$ is the cross section for excitation of the ^1D state from the ^3P ground state by impact of electrons with energy ε, and v is the electron velocity corresponding to the energy ε.

The third term on the right of (1) represents the natural decay of the ^1D state by emission of the 6300 and 6364A wavelength transitions; τ_n has been calculated to be 110 sec [Garstang, 1951]. The fourth term represents quenching by collisions with ambient molecules. Laboratory measurements of k_q [Clark and Noxon, 1972; Noxon, 1970; Young et al., 1968] indicate that N_2 and O_2 are comparably effective; thus since $[O_2] \sim 0.1\,[N_2]$ over the altitude range of interest, 220-300 km, we have simplified the analysis by lumping both processes into a single term, $1.1\, k_q\, [N_2]\, [^1D]$. (Electron quenching of $O(^1D)$ with a coefficient

1.7×10^{-9} cm^3/sec [Seaton, 1955] is negligibly slow at F-region electron concentrations.)

The final term on the right of (1) represents the diffusion of the excited atoms with diffusion coefficient, D_x, and can be shown to be relatively unimportant on the time scales, 10-90 sec, of interest here. Thus, the $O(^1D)$ concentration is governed by a continuity equation consisting of two source terms which are sensitive to the electron energy distribution produced by the rf heating, and a volume loss term which may be written as $(1/\tau')$ $[^1D]$, where

$$(1/\tau') = (1/\tau_n) + k_q [N_2] \equiv (1/\tau_n) \{1/D(z)\} \qquad (4)$$

where D(z) is the so-called Stern-Volmer factor (see, for example Mitchell and Zemansky, [1961]).

The source terms Q_r and Q_x change in opposite ways with electron heating. The recombination coefficient between O_2^+ ions and electrons has been shown [Mehr and Biondi, 1969] to vary approximately as $T_e^{-0.6}$ for the electron temperatures of interest, leading to a decrease in Q_r with increase in T_e. The impact excitation of oxygen atoms requires electrons with energies exceeding ~ 2 eV; if the electron energy distribution remains nearly Maxwellian during rf heating, this leads to a sharp electron temperature dependence for Q_x. An estimate of the expected 6300A surface brightness from the F-region as a function of electron temperature has been made by Carlson [1969] using the calculated cross section for excitation to the ^1D state [Smith, et al., 1967; Seaton, 1953]. He assumed that a layer 150 km thick and at a constant density appropriate to 350 km altitude was excited by electrons heated to a temperature

T_e. In the present paper, the surface brightness attributable to direct excitation at an altitude of 300 km has been calculated from the expression

$$I = \int_{z_1}^{z_2} Q_x(z)\, D(z)\, dz, \qquad (5)$$

assuming that the electron energy distribution $f(\varepsilon)$ in (3) is characterized by a constant elevated temperature T_e over the heated volume between z_1 and z_2. Numerical integrations of (5), using an appproximate fit to the calculated excitation cross section and a model atmosphere given in Table I have been carried out, with the results shown in Figure 2. The thickness of the uniformly heated layer is the parameter on these curves; Carlson's estimate (which has no quenching or altitude dependent densities) evidently overestimates the intensity enhancement.

This "intensity enhancement" produced by impact excitation is partly offset by the "intensity suppression" produced by the decreased dissociative recombination rate. In the earlier analysis of the intensity suppression signals [Biondi, et al., 1970] it was assumed that the whole of the nightglow emitting layer within the field of view of the photometer was suppressed in intensity in estimating the change of T_e produced by the heating transmitter. However, both backscatter measurements [Gordon, et al., 1971] and our spatial scans indicate that the heated region is sometimes rather restricted in altitude. Thus the rise in T_e required to produce the observed suppression signals may be significantly larger than originally estimated. Of more importance to the present paper, restricting the affected region of the ionosphere to a small fraction of the 6300A emitting layer leads to conditions such that the intensity enhancement signals should strongly outweigh the suppression effect, thus

simplifying the analysis. In the Discussion section we shall show why diffusion of the heated electrons along the earth's magnetic field lines leads to only a modest spreading in altitude of the enhanced emission zone.

Apparatus

The instrument used in this work is a two-channel spatial scanning photometer with an automatic control and data recording system, as shown schematically in Figure 3. Two identical photometers are used for simultaneous observation at two wavelengths. A mirror driven about two axes is used to effect a spatial scan. Pulses from the phototube are counted and recorded on 1/2-inch computer-compatible digital magnetic tape.

Each of the photometers consists of an interference filter, lens, and photomultiplier detector with an aperture to define the field of view (6°). Four interference filters of half width $\sim$ 11A and peak transmission $\sim$ 65% are provided, two for each photometer. One photometer employs either a 6300A or a 5552A filter, while the other photometer employs either a 6333A or a 5577A filter. This permits observation of the red and green lines simultaneously, or one of the lines and a nearby spectral region to be used as a background intensity monitor.

The lens is a 2-inch diameter 5 inch focal length achromat. Light coming through the lens is focussed on the photocathode of an EMI 9558A phototube. The 9558 tube is selected for low dark current and high red sensitivity. A 1/2-inch aperture is placed just before the photocathode, defining the field of view of the photometer. In order to eliminate the electrons from the area of the 2-inch photocathode outside the aperture, a cylindrical magnetic lens is placed in front of the photocathode. The diverging magnetic field carries

electrons from the edge of the photocathode to the walls of the tube, avoiding the multiplying surfaces. Thus the electrons in the center are the only electrons to be multiplied and counted. The photomultiplier tube, aperture, and magnet are contained within a PFR model TE102TS thermoelectric cooler, which reaches a temperature of about $-15^{\circ}C$, close to the optimum temperature for the phototubes ($-20^{\circ}C$).

The scanning mirror is held on a frame which is movable about an axis in the plane of the mirror (y axis). The mirror frame is mounted on ball bearings on a secondary frame which is movable about the x axis (perpendicular to the y axis and on the axis of the photometers). A stepping motor is used to drive each axis. The stepping motor for the y axis is placed as close as possible to the x axis in order to minimize the moment of inertia about the x axis. The entire photometer and mirror system is mounted an an azimuth-elevation mount, so that it can be aimed at any point in the sky.

The spatial scan and the data acquisition intervals are controlled by a 100 kHz crystal clock. The mirror position is changed, typically at 1 or 2 sec intervals, by a programmed series of pulses to each stepping motor to achieve a pre-selected scan step. A raster scan is used in which the mirror axis drives are programmed to provide a repeated search pattern, typically 3 x 3 elements, with an element separation of $\sim 8^{\circ}$. At each mirror position change, the photomultiplier counts accumulated in the counters are transferred to the Kennedy Model 1600H incremental tape recorder and to a Brush Model 220 chart recorder in analogue form. In addition to the two 18 bit counter words, the time, filter-in-use, and scanning mirror position information are placed on the tape.

Absolute intensity calibration of the photometer is provided by a low brightness phosphor source activated by radioactive C^{14}. This source has been

calibrated by E. Marovich at NOAA.

Measurements

The measurements were carried out in conjunction with the Institute for Telecommunication Science's Platteville heating transmitter (40.18°N, 104.73°W) located near Denver, Colorado. The optical photometer was located near Erie, Colo., approximately 26 km WSW of the transmitter (refer to Figure 1). An ionosonde was operated by ITS at the Erie site, producing complete ionograms about every half minute, thus providing electron density vs altitude profiles to correlate with the photometer observations.

Most of the observations reported in the present paper were made with the transmitter's antenna propagating the O-mode polarization. Such propagation evidently leads to sufficiently strong r-f fields at the absorption point in the F_2 region to trigger strong plasma instabilities which in turn produce a strongly non-Maxwellian electron energy distribution [Perkins and Kaw, 1971]. There is a sufficient number of energetic electrons ($\geq$ 2 eV energy) to produce significant impact excitation of the O atoms to the ^1D state, leading to observable 6300A intensity enhancements.

Examples of the nightglow enhancements observed during September and October 1970 are given in Figures 4 and 5. The absolute intensities were obtained by substracting from the 6300A channel count rate the continuum contribution determined from the 6333A background channel. (The 6333A channel showed no variation in intensity with the turning on and off of the transmitter.)

Intensity enhancements of $\sim$ 15-40% over the ordinary 6300A nightglow values were noted on these nights. Reference to Figure 2 indicates that, for a thin emitting layer, an electron temperature of 2500°K or more is required to produce

the observed effect. Such a large temperature rise is not expected for ordinary collisional heating of the electrons by the electromagnetic wave (deviative absorption), lending support to the plasma wave heating hypothesis.

The data of Figure 4 represent intensities measured at the central scan position of a 3 x 3 scan pattern. With a dwell time of 2 sec. at each position, the data points are therefore spaced 18 sec. apart in time, leading to some uncertainties in the determinations of the ^1D quenching lifetimes. It is interesting to note that at ~ 2132 MDT, when the critical frequency f_oF_2 dropped below the heating frequency f, an abrupt fall in intensity was observed, indicating that the production of energetic electrons decreased sharply, with a consequent decrease in excitation of oxygen atoms to the ^1D state. At the next transmitter turn on, at ~ 2142 MDT, no intensity enhancement was observed (instead there was an indication of a weak intensity suppression) suggesting that significant production of > 2 eV electrons had ceased. The implications of this apparent change in the excitation of the electrons by the heating wave will be discussed in a later paper.

The data of 30 October 1970 presented in Figure 5 were obtained with the photometer aimed at one point in the sky and a dwell time of 1 sec/point; thus the data appear dense on the time scale of the figure and provide a sufficient number of points to determine the ^1D lifetime accurately. In the 30 October experiment, the sensitivity of the intensity enhancement to transmitter power was being studied, as indicated by the power levels under each enhancement. On the third cycle the transmitter failed shortly after turn-on.

For completeness we indicate in Figure 6 the very different behavior observed on 30 September 1970 when X-mode propagation was used at the same transmitter power levels. A 6 min. on - 6 min. off cycle was used, and instead

of an enhancement of tens of Rayleighs, a transient decrease of ∿ 2 Ray. was noted when the transmitter was turned on, with a comparable transient increase when the transmitter was turned off. This behavior is consistent with our earlier observations and analysis of the X-mode heating effect [Biondi, et al., 1970]. The data in Figure 6 were obtained by coherently summing the points obtained during the four on-off cycles between 2100 and 2148 MDT. This procedure reduced slightly the statistical fluctuations in the determination of the ∿ 2 Ray. modulation of the 110 Ray. nightglow intensity.

Discussion

The data of Figures 4, 5, and 6 may be used to determine effective lifetimes of the $O(^1D)$ atoms at various heights in the F_2 region. The most accurate determinations are obtained from the 1 sec. per point measurements of Figure 5. The observations during the latter portion of this run (beyond ∿ 1840 MST) were degraded by a thick cloud layer which drifted into the field of view.

For the case of intensity enhancements produced by electron impact excitation of oxygen atoms it is readily shown that if the heated electrons reach a terminal energy in a time short compared to the $O(^1D)$ lifetime given by (4), the 6300A intensity approaches the new equilibrium value with a time constant equal to this lifetime. Thus the data of Figure 5 have been analyzed by taking differences between the observed intensity at each instant and the equilibrium value it is approaching. The results for the first turn-on and turn-off of the transmitter are plotted in Figure 7. It will be seen that the data fall on exponential decay curves over an order of magnitude change of

intensity and that the two time constants are in good agreement. Similar intensity difference curves for the second on-off cycle (at 1.5 Mw power) of the transmitter yield time constants of (11.3 ± 1) and (12.0 ± 1) sec. Much greater scatter in the intensity difference points is noted during the later transmitter on-off cycles (at 1.28 and 1.21 Mw) as a result of interference from the buildup of clouds. In spite of this difficulty, a time constant of $\sim$ (13 ± 4) sec. is obtained for these later transients, in satisfactory agreement with the results from the earlier transients.

The observation of an exponential decay over an order of magnitude change in intensity difference suggests that at most a small range of $O(^1D)$ lifetimes is associated with the 6300A enhanced emission layer. This in turn implies that the enhanced emission layer is localized to an altitude range substantially less than a scale height of the N_2 molecules ($\sim$ 27 km), since the $\sim$ 13 sec ^1D lifetime must be almost completely determined by molecular quenching. Let us now see if such localization is consistent with the expected diffusion of the exciting electrons upward and downward along the magnetic field lines.

The small group of $\gtrsim$ 2 eV electrons produced by the instability heating will lose energy by long range electron-electron interactions with the large number of near-thermal electrons in the "body" of the energy distribution. At an electron density of 3.5×10^5 cm^{-3} (corresponding to plasma resonance with the transmitter at f = 5.3 MHz), the fast electrons lose appreciable energy as a result of electron-electron interactions in less than 1 sec. [Swartz, et al., 1971]. Collisions with ambient N_2 molecules at 225 km (the altitude of transmitter energy absorption for these data) lead to a comparable relaxation-time [Frost and Phelps, 1962].

We assume that the spread of these fast electrons is governed by ambipolar diffusion; that is, the positive ions must follow in order to maintain near-

neutrality. (Possible interchange at a free diffusion rate of fast electrons at one altitude with slow electrons at another altitude is neglected.) If we use a Spring/Fall model atmosphere with $T_{exo} = 950^{o}K$* [U.S. Standard Atmosphere Supplements, 1966] to obtain the concentration of the various neutral constituents (these values are quite close to those given in Table I), it is possible to estimate the ambipolar diffusion coefficient for the fast electrons from the known ion mobilities of the various positive ion/neutral molecule constituents, e.g. O^{+} in N_2. (The normalized mobilities are in the range $\mu_o \sim 2\text{-}3$ $cm^2/V\text{-}sec$ [McDaniel, 1964].) At 225 km, an ambipolar diffusion coefficient for the electrons of $< 10^{10}$ cm^2/sec is obtained, with the result that the mean distance a fast electron diffuses along the magnetic field before losing its energy, $\bar{z} \sim (2 D_a \tau)^{1/2}$, is substantially less than 1 km.

The diffusion of the $O(^1D)$ atoms away from their point of creation can also be shown to be small at the 225 km altitude of enhancement. The diffusion coefficient for the excited atoms at this altitude may be estimated from momentum transfer and excitation transfer cross section data for metastable atoms [Massey, 1971], leading to a value $D_x \sim 10^9$ cm^2/sec. Consequently during its $\sim$ 13 sec lifetime before quenching, an $O(^1D)$ atom diffuses the order of 1 km from its point of creation.

Thus, unless the process which produces energetic electrons extends over an appreciable altitude range, the 6300A radiation originating from electron impact excitation of oxygen atoms should be localized in altitude to consider-

---

*This value was chosen on the basis of a determination by G. Hernandez of a 6300A doppler temperature of $(950 \pm 30)^{o}K$ in interferometric observations from Fritz Peak on the same evening.

ably less than a scale height of the quenching molecules. This conclusion is in harmony with our finding of a single $O(^1D)$ lifetime associated with the enhanced emission region near 225 km. However at 300 km, where the diffusion coefficients for the excited atoms and the electrons are almost an order of magnitude larger and the $O(^1D)$ lifetime against quenching is substantially longer, the enhanced emission layer may be spread in altitude, even if the exciting electrons are produced at a well-defined altitude.

Average lifetimes of the $O(^1D)$ atoms have also been determined from the 6300A intensity change data of Figure 4. Here the decay of ionospheric electron density during the course of the observations resulted in an appreciable change in the altitude of energy deposition by the 5.3 MHz heating wave (from 260-300 km). Since a given region of the ionosphere was under observation only once every 18 seconds during the 9 point spatial scan, the inferred lifetimes exhibit rather large uncertainties, especially those at the lower end of the 30-90 sec range of the measurements. Accordingly, lifetimes were determined for each of the 9 points in the spatial scan which gave measurable intensity changes. The results of the lifetime determinations are plotted in Figure 8 for each of the eleven 6300A intensity changes produced during the period between 2030 and 2132 MST. (Larger diameter circles indicate more confidence in the inferred lifetimes as a result of less scatter in the intensity difference curves.) The altitudes indicated on the figure are the heating wave reflection heights (where $f = f_p$) determined from ionograms taken at the indicated times. It will be seen that, at a given time, rather different lifetimes are inferred from the different observation points in the spatial scan, perhaps as a result of spreading of the enhanced emission layer along the magnetic field lines in these higher altitude ($\sim$ 280 km) observations.

The data of Figures 7 and 8 may be used to infer an in-situ quenching coefficient for $O(^1D)$ atoms by the ambient N_2 and O_2 molecules. From the model atmosphere given in Table I (corrected to 950°K), at the heating wave reflection height appropriate to the data of Figure 7, i.e. 225 km, the N_2 density is 1.6×10^9 cm^{-3} and the O_2 density 1.5×10^8 cm^{-3}. Thus, the 13 sec lifetime found in Figure 7 implies a quenching coefficient, $k_q = 4.4 \times 10^{-11}$ cm^3/sec.

As a result of the scatter of the data in Figure 8, a different analysis procedure was adopted. Using the reflection height data given in the figure together with the N_2 and O_2 densities from the model atmosphere of Table I (corrected to $T_{exo} = 950°K$), a family of curves of $O(^1D)$ lifetime as a function of altitude (observation time) was constructed with k_q as a parameter. These curves are represented by the solid lines in Figure 8. It will be seen that, for the more reliable lifetime determinations, a quenching coefficient between 3 and 7 $\times 10^{-11}$ cm^3/sec fits most of the data. These values, covering the 260–300 km region are in quite satisfactory agreement with the more accurately determined value at 225 km.

Finally, the data points corresponding to the intensity suppression transient given in Figure 6 have been analyzed following the procedure given by Biondi et al. [1970]. The solid line is the expected form of the transient if the $O(^1D)$ lifetime is taken to be 40 sec and the dissociative recombination lifetime 70 sec. The heating wave reflection height for these measurements was determined from an ionogram to be 235 km. Using the appropriate densities from the model (corrected to $T_{exo} = 1030°K$), one obtains a value $k_q \sim 2 \times 10^{-11}$ cm^3/sec, in acceptable agreement with the value 4.4×10^{-11} cm^3/sec determined previously, considering the large scatter in the data associated with the intensity suppression transients.

Taken together the 6300A intensity enhancement data yield a value k_q = $(4.4 \pm {}^{2}_{1}) \times 10^{-11}$ cm^3/sec at 950°K, in agreement with the laboratory value $k_q(N_2) = (5 \pm 2) \times 10^{-11}$ cm^3 at 300°K [Clark and Noxon, 1972; Young et al., 1968]. Further, our result is consistent with the other, less direct in-situ determination of $O(^1D)$ quenching by Peterson and van Zandt [1969]. These authors expressed their results in terms of an inferred quenching frequency at a reference height of 120 km. Using the value $k_q = 4.4 \times 10^{-11}$ cm^3/sec determined from our best data at 225 km, together with the molecular concentrations at 120 km, $[N_2] = 4.0 \times 10^{11}$ cm^{-3} and $[O_2] = 0.8 \times 10^{11}$ cm^{-3} [U.S. Standard Atmosphere Supplements, 1966], we obtain a quenching frequency at 120 km, $\nu = k_q ([N_2] + [O_2]) = 21$ sec^{-1}, in excellent agreement with Peterson and van Zandt's value of 20 sec^{-1}, which they believed accurate only to a factor of two.

Conclusions

The present paper has presented some initial results obtained by the use of powerful ground-based transmitters to produce controlled changes in the ionosphere. The technique offers the possibility of studying a wide variety of phenomena ranging from observations of plasma waves and their interaction with ionospheric electrons to in-situ determinations of the nature and the rates of the important ionospheric atomic collision processes.

In the present case the determination of the $O(^1D)$ quenching coefficient to be $(4.4 \pm {}^{2}_{1}) \times 10^{-11}$ cm^3/sec at $\sim$ 950°K rests on the assumption that the enhanced 6300A emission layer is localized to the region where the heating electromagnetic wave is strongly absorbed, in agreement with our present understanding of the electron heating mechanism. However, if the exciting electrons are produced at altitudes appreciably above the point at which $f = f_p$, the deter-

mination represents a lower bound on the quenching coefficient. In this case, the observation of a single decay time for the 6300A intensity variation implies that the acceleration mechanism results in production of the exciting electrons over a rather limited altitude range. Future studies in collaboration with J. C. Hazlett of NOAA will involve triangulation measurements to obtain more information on the height distribution of the enhanced 6300A intensity region.

The authors are indebted to R. D. Hake for his contributions to the design and construction of the photometer, to J. C. Hazlett of NOAA for his assistance with the field-site preparation and operation, and to W. Utlaut, E. J. Violette and J. Carroll of ITS for their cooperation in the operation of the Platteville transmitter. This research was supported, in part, by the Advanced Research Projects Agency, Department of Defense, and was monitored by the U. S. Army Research Office (Durham) under Contract No. DA-31-124-ARO-D-440.

Table I Model Atmosphere Composition† and Predicted $O(^1D)$ Lifetimes

Alt(km)	$[N_2](cm^{-3})$	$[O_2](cm^{-3})$	$[O](cm^{-3})$	$n_e(cm^{-3})$	$\tau(^1D)(sec)$
180	7.86(9)*	9.39(9)	5.38(9)	7.74(3)	1.4
200	4.15(9)	4.55(8)	3.70(9)	3.90(4)	2.6
220	2.19(9)	2.20(9)	2.55(9)	1.08(5)	4.8
240	1.16(9)	1.07(8)	1.75(9)	2.00(5)	8.8
260	6.10(8)	5.17(7)	1.20(9)	2.83(5)	15.6
280	3.22(8)	2.51(7)	8.28(8)	3.34(5)	26.3
300	1.70(8)	1.21(7)	5.70(8)	3.50(5)	41.0
320	8.97(7)	5.89(6)	3.92(8)	3.38(5)	58.2
340	4.74(7)	2.85(6)	2.70(8)	3.09(5)	74.9
360	2.50(7)	1.38(6)	1.85(8)	2.72(5)	88.2

*Read as 7.86×10^9

†Neutral densities are based on $T_{exo} = 1000^oK$ in a Spring/Fall Model [U.S. Standard Atmosphere Supplements, 1966]. Electron densities have been calculated using a Chapman layer [Chamberlain, 1961] with a peak concentration of 3.5×10^5 cm^{-3} at 300 km and a scale height of 60 km.

REFERENCES

Biondi, M. A., D. P. Sipler, and R. D. Hake, Jr., Optical (λ6300) detection of radio frequency heating of electrons in the F region, J. Geophys. Res., 75, 6421, 1970.

Carlson, H. C., private communication, 1969.

Chamberlain, J. W., PHYSICS OF THE AURORA & AIRGLOW, Academic Press, New York, 1961.

Clark, I. D. and J. F. Noxon, Optical emission $O(^1D)$ and $O_2(b^1\Sigma_g)$ in ultraviolet photolysis of O_2 and CO_2,II, J. Chem. Phys., in press, 1972.

Frost, L. S. and A. V. Phelps, Rotational excitation and momentum transfer cross sections for electrons in H_2 and N_2 from transport coefficients, Phys. Rev., 127, 1621, 1962.

Garstang, R. H., Energy levels and transition probabilities in p^2 and p^4 configurations, Monthly Notices, Roy. Astron. Soc., 111, 115, 1951.

Gordon, W. E., R. Showen and H. C. Carlson, Ionospheric heating at Arecibo: first tests, J. Geophys. Res. 76, 7808, 1971.

McDaniel, E. W., COLLISION PHENOMENA IN IONIZED GASES, John Wiley and Sons, New York, 1964.

Massey, H.S.W., ELECTRONIC AND IONIC IMPACT PHENOMENA, VOL. 3, Oxford Univ. Press, London, England, 1971.

Mehr, F. J. and M. A. Biondi, Electron temperature dependence of recombination of O_2^+ and N_2^+ ions with electrons, Phys. Rev. 181, 264, 1969.

Meltz, G. and R. E. LeLevier, Heating the F region by deviative absorption of radio waves, J. Geophys. Res. 75, 6406, 1970.

Mitchell, A. C. G., and M. W. Zemansky, RESONANCE RADIATION AND EXCITED ATOMS, Cambridge University Press, Cambridge, 1961.

Noxon, J. F., Optical emission from $O(^1D)$ and $O_2(b^1\Sigma_g)$ in ultraviolet photolysis of O_2 and CO_2, J. Chem. Phys., 52, 1852, 1970.

Perkins, F. W. and P. K. Kaw, On the role of plasma instabilities in ionospheric heating by radio waves, J. Geophys. Res. 76, 282, 1971.

Peterson V. L. and T. E. van Zandt, $O(^1D)$ quenching in the ionospheric F-region, Planet. Space Sci., 17, 1725, 1969.

Seaton, M. J., The Hartree-Fock equations for continuous states with applications to electron excitation of the ground configuration terms of OI, Phil. Trans. Roy. Soc. London A245, 469, 1953.

Seaton, M. J., The calculation of cross-sections for excitation of forbidden atomic lines by electron impact, J. Atmos. Terr. Phys., Special Supplement, 5, 289, 1955.

Sipler, D. P. and M. A. Biondi, Determination of the $O(^1D)$ quenching coefficient in the F region, Trans. Am. Geophys. Union, 52, 883, 1971.

Smith, K., R. J. W. Henry and P. G. Burke, Calculations on the scattering of electrons by atomic systems with configurations $2p^8$, Phys. Rev. 157, 51, 1967.

Swartz, W. E., J. S. Nisbet, and A. E. S. Green, Analytic expression for the energy-transfer rate from photoelectrons to thermal electrons, J. Geophys. Res., 76, 8425, 1971.

U. S. Standard Atmosphere Supplements, Supt. Documents, U.S. Government Printing Office, Wash., D. C., 1966.

Utlaut, W. F., An ionospheric modification experiment using very high power, high frequency transmission, J. Geophys. Res., 75, 6402, 1970.

Utlaut, W. F., and R. Cohen, Modification of the ionosphere with intense radio waves, Science, 174, 245, 1971.

Young, R. A., G. Black and T. G. Slanger, Reaction and deactivation of $O(^1D)$, J. Chem. Phys., 49, 4758, 1968.

Zipf, E. C., The dissociative recombination of O_2^+ ions into specifically identified final atomic states, Bull. Am. Phys. Soc., 15, 418, 1970.

FIGURE CAPTIONS

Figure 1 Geometry of the Ionospheric Modification Experiment.

Figure 2 Calculated 6300A intensities as a function of electron temperature. The solid curves refer to an emission altitude of 300 km and various emitting layer thicknesses (see text for details).

Figure 3 Simplified diagram of the dual channel scanning photometer apparatus.

Figure 4 6300A intensity enhancements produced by ordinary polarization waves on 25 September 1970. The critical frequency f_oF_2 decreased below the transmitter frequency at ~ 2132 MDT.

Figure 5 6300 intensity enhancements as a function of heating transmitter power on 30 October 1970.

Figure 6 6300 intensity suppression transients produced by extraordinary polarization waves on 30 September 1970. The data from four transmitter on-off cycles have been coherently summed to obtain the points shown in the figure.

Figure 7 Determination of the time constant for $O(^1D)$ atom decay from the intensity enhancement data of Figure 5. The 6300A emission height is 225 km (see text for details).

Figure 8 Decay time constants as a function of altitude deduced from the data of 25 September 1970. The larger circles indicate more accurate determinations.

Figure 1

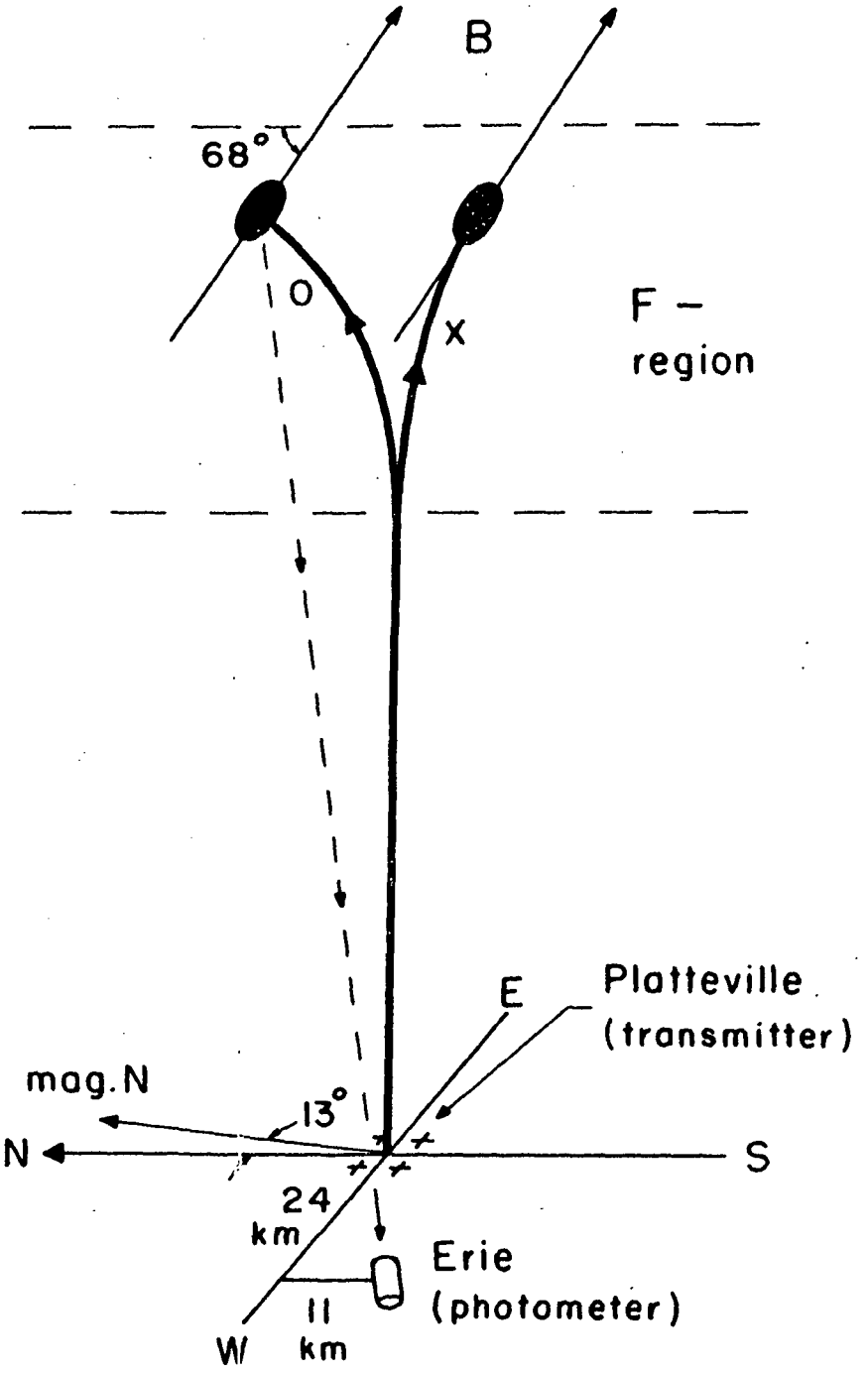
B
68°
O
X
F –
region
E
Platteville
(transmitter)
mag.N
13°
N
S
24
km
Erie
(photometer)
11
km
W

Figure 2

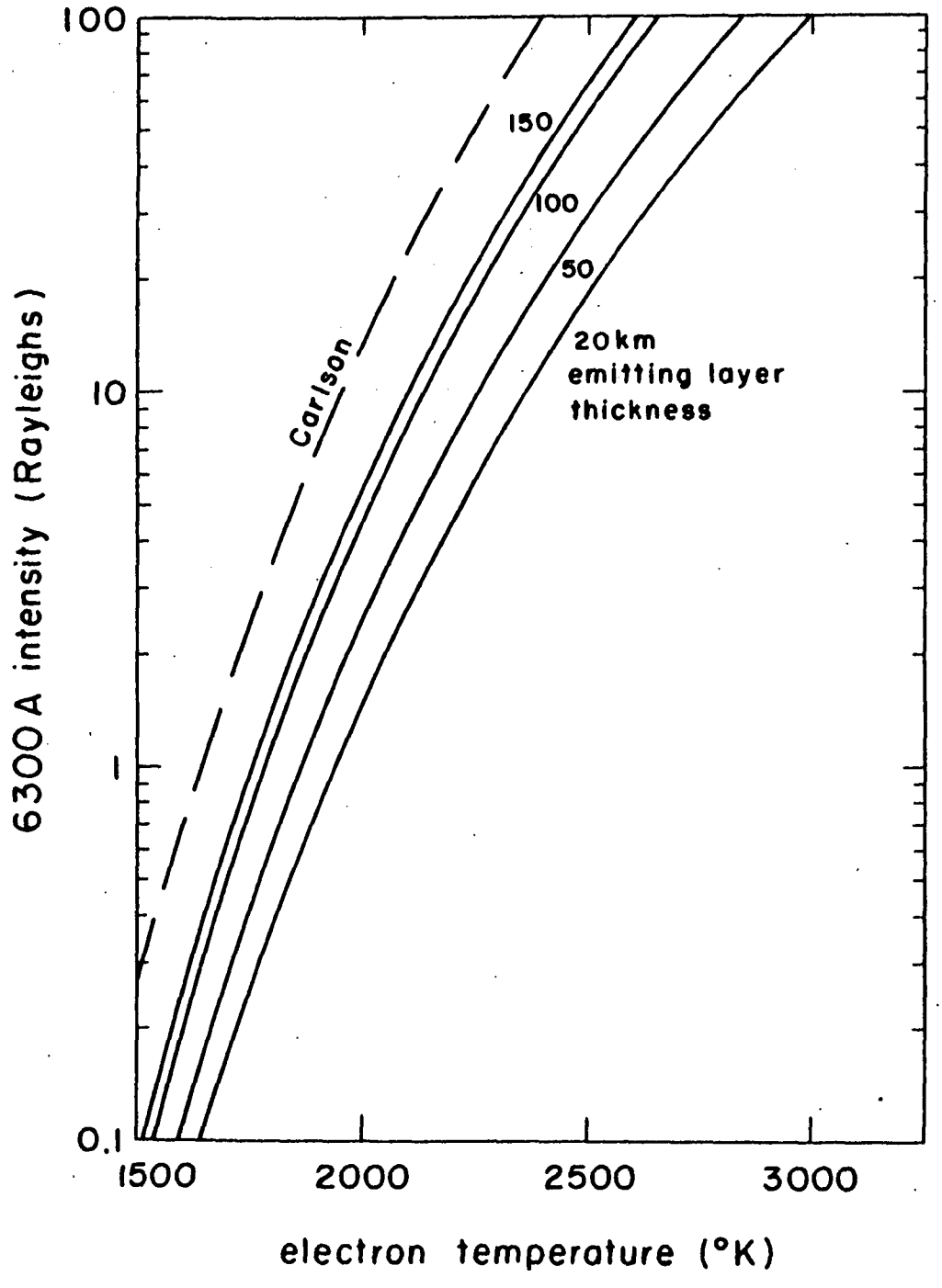
100
10
1
0.1
6300 A intensity (Rayleighs)
150
100
50
20km
emitting layer
thickness
Carlson
1500
2000
2500
3000
electron temperature (°K)

Figure 3

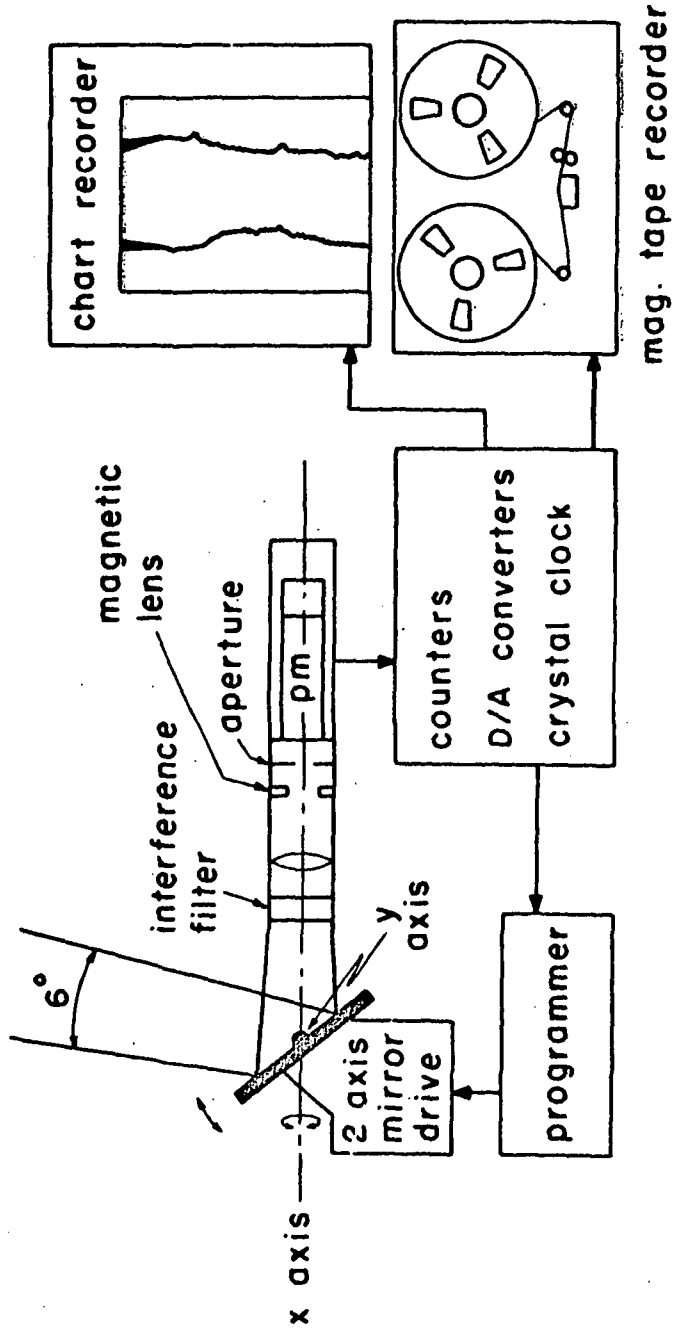
chart recorder
mag. tape recorder
counters
D/A converters
crystal clock
programmer
magnetic lens
aperture
pm
interference filter
y axis
6°
2 axis mirror drive
x axis

Figure 4

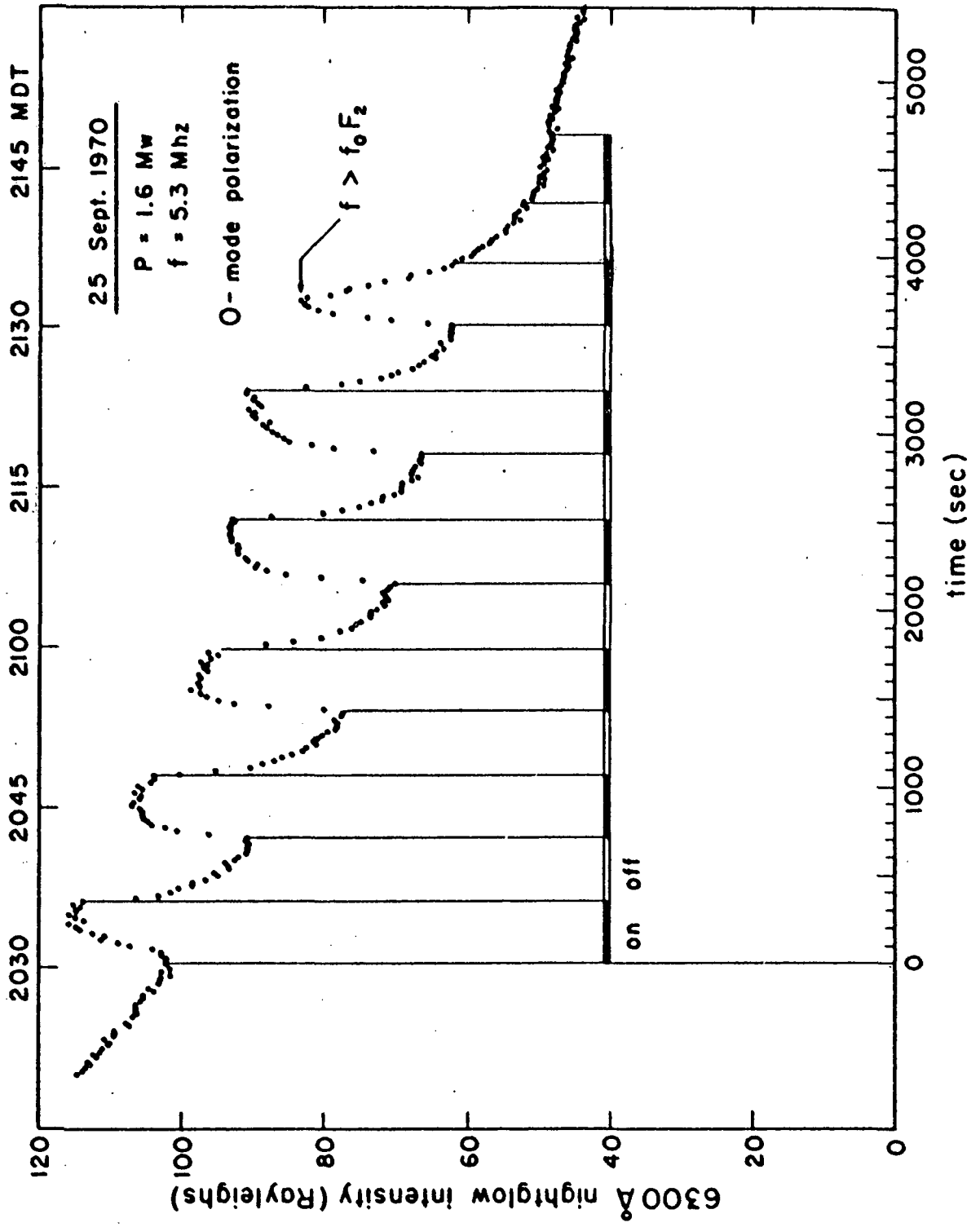
25 Sept. 1970
P = 1.6 Mw
f = 5.3 Mhz
O-mode polarization
f > f0F2
on off
6300 Å nightglow intensity (Rayleighs)
time (sec)
2030
2045
2100
2115
2130
2145 MDT
0
20
40
60
80
100
120
0
1000
2000
3000
4000
5000

Figure 5

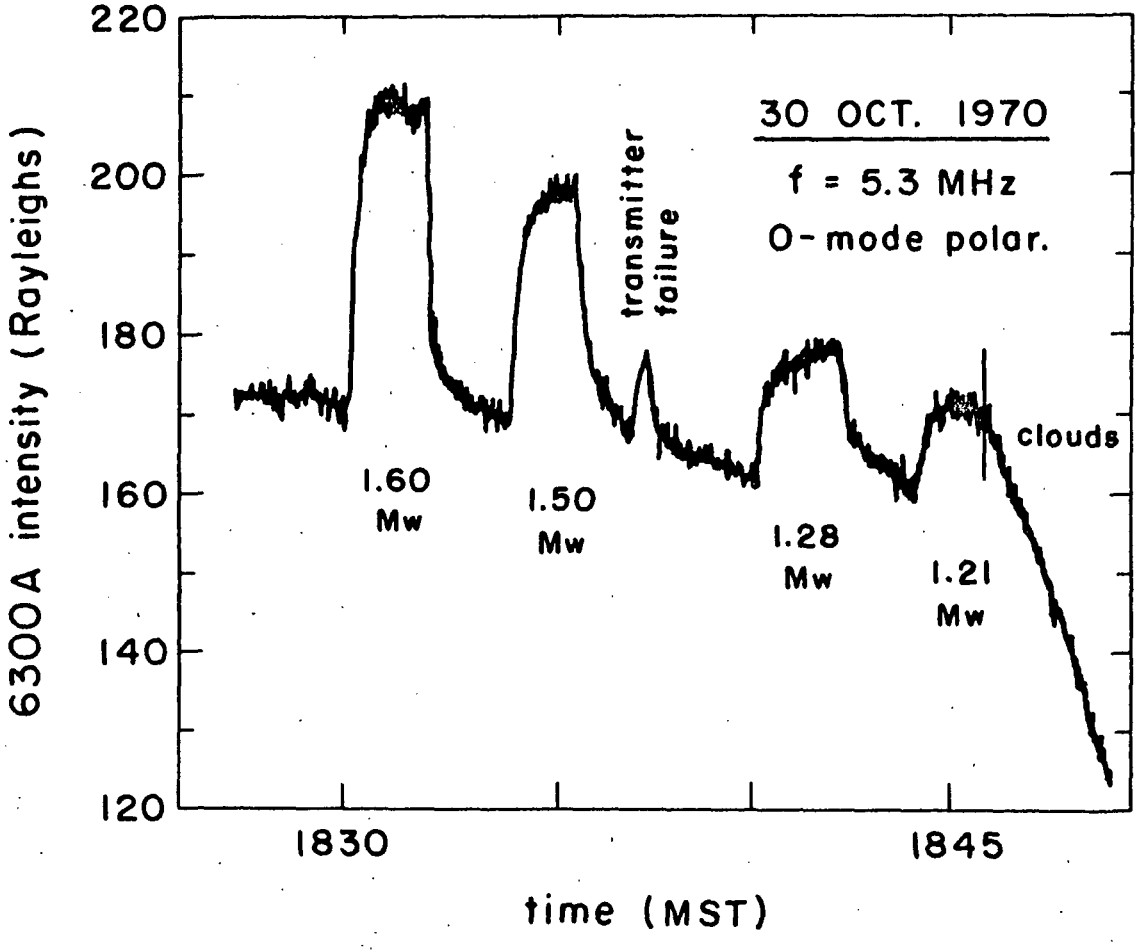
6300A intensity (Rayleighs)
220
200
180
160
140
120
1830
1845
time (MST)
30 OCT. 1970
f = 5.3 MHz
O-mode polar.
transmitter failure
1.60 Mw
1.50 Mw
1.28 Mw
1.21 Mw
clouds

Figure 6

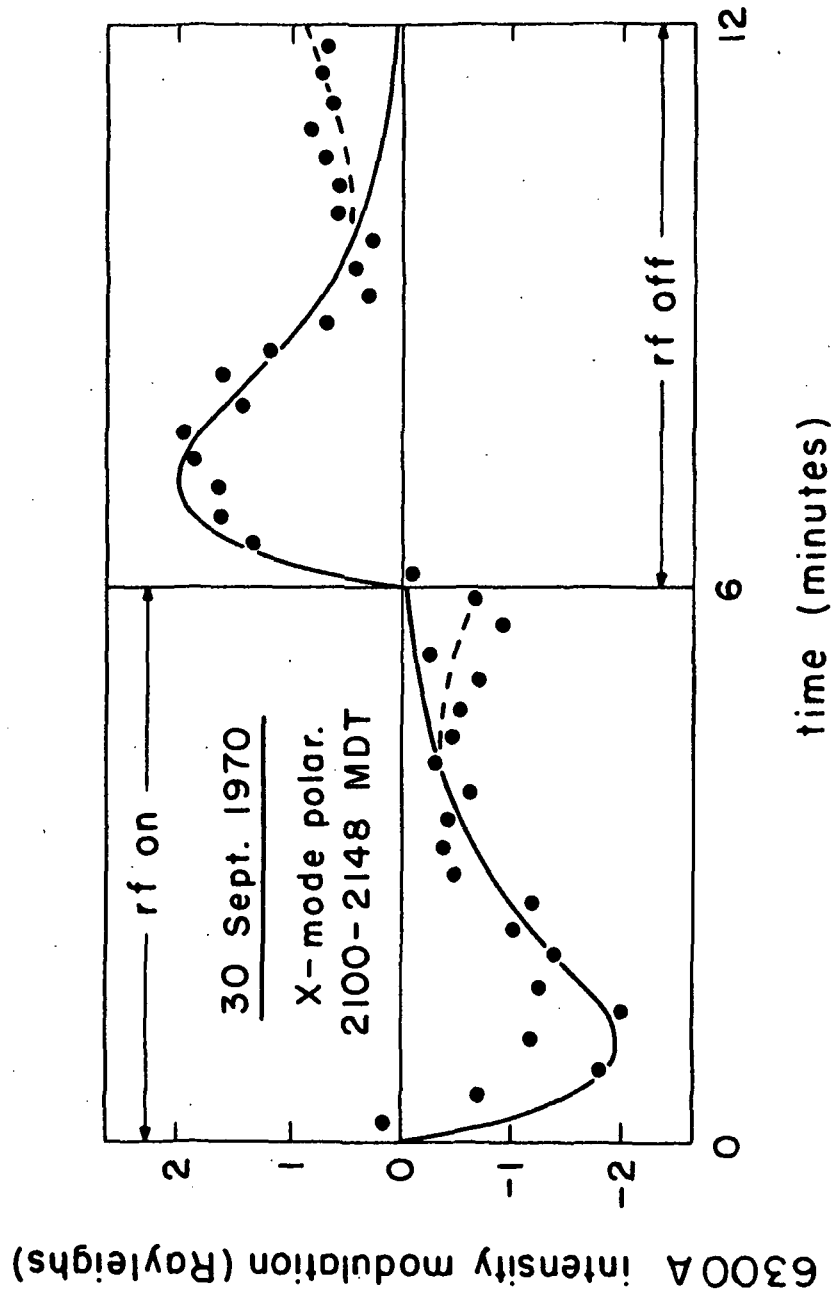
6300 A intensity modulation (Rayleighs)
2
1
0
-1
-2
0
6
12
time (minutes)
rf on
rf off
30 Sept. 1970
X-mode polar.
2100-2148 MDT

Figure 7

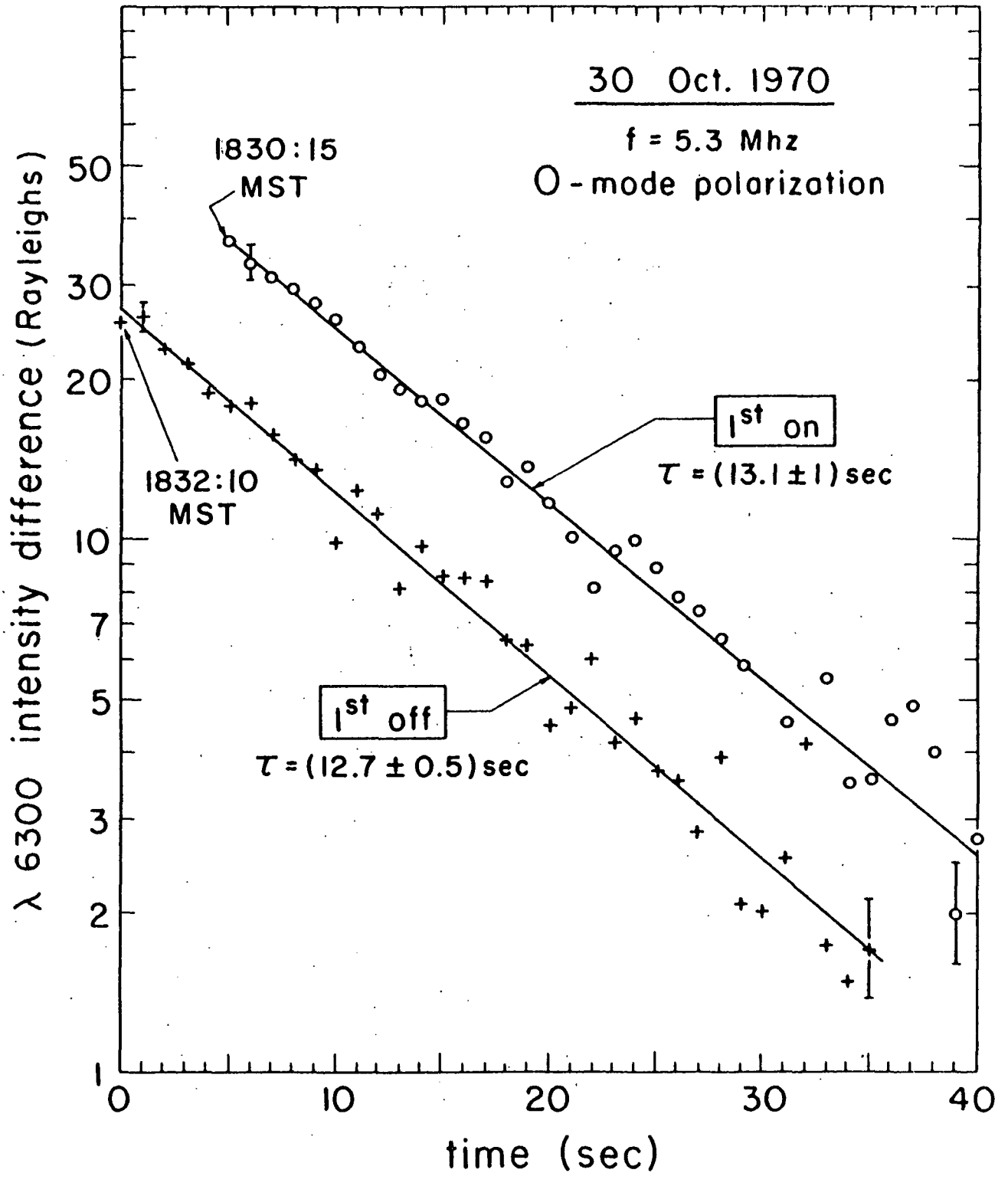
30 Oct. 1970
f = 5.3 Mhz
O-mode polarization
1830:15
MST
1832:10
MST
1st on
τ = (13.1 ± 1) sec
1st off
τ = (12.7 ± 0.5) sec
λ 6300 intensity difference (Rayleighs)
time (sec)
50
30
20
10
7
5
3
2
1
0
10
20
30
40

Figure 8

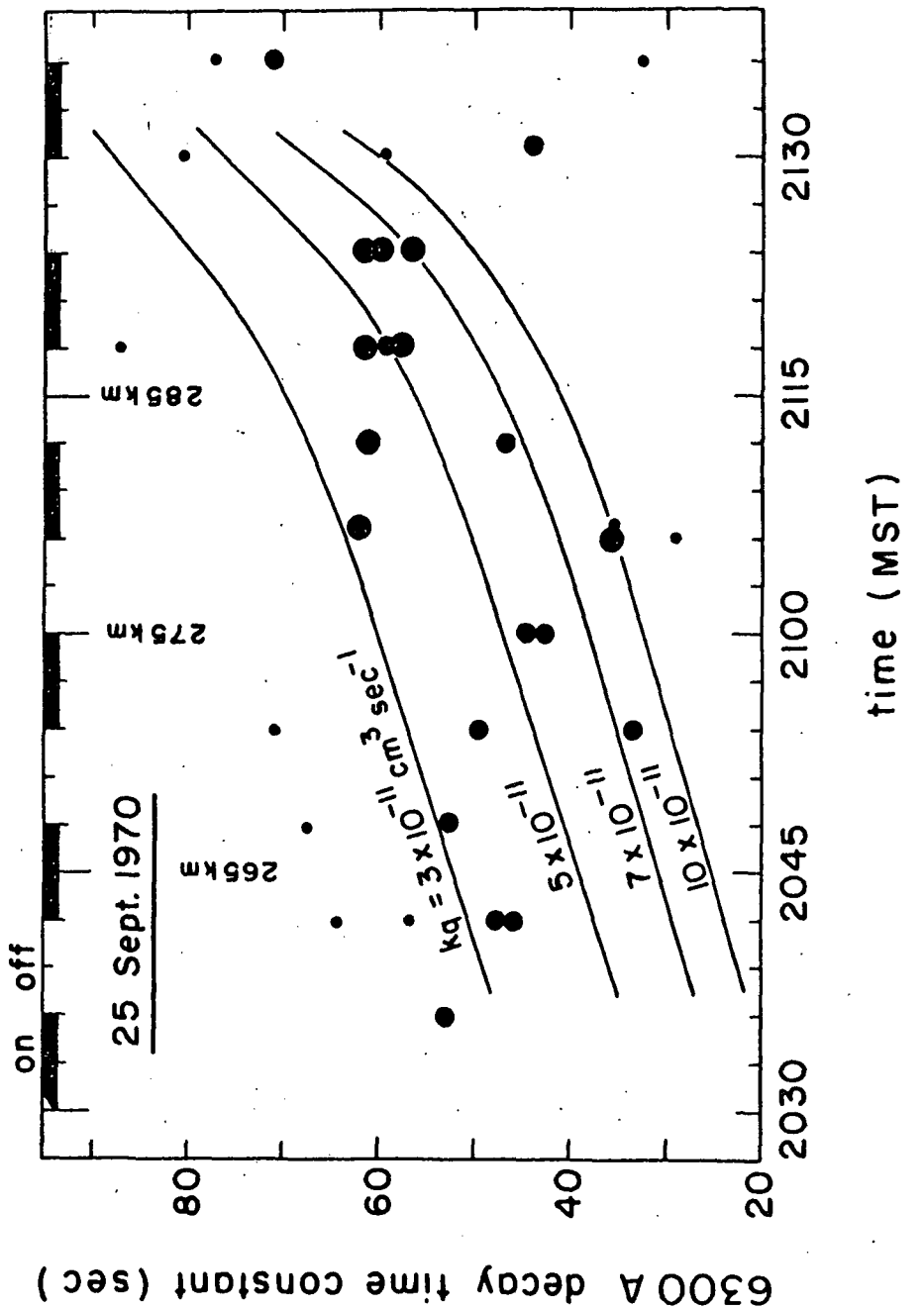
6300 Å decay time constant (sec)
80
60
40
20
2030
2045
2100
2115
2130
time (MST)
on off
25 Sept. 1970
265km
275km
285km
kq = 3x10^-11 cm^3 sec^-1
5x10^-11
7x10^-11
10x10^-11